

Evidence of Rocky Planetesimals Orbiting Two Hyades Stars

J. Farihi^{1*}†, B. T. Gänsicke², D. Koester³

¹*Institute of Astronomy, University of Cambridge, Cambridge CB3 0HA*

²*Department of Physics, University of Warwick, Coventry CV4 7AL*

³*Institut für Theoretische Physik und Astrophysik, University of Kiel, 24098 Kiel, Germany*

ABSTRACT

The Hyades is the nearest open cluster, relatively young and containing numerous A-type stars; its known age, distance, and metallicity make it an ideal site to study planetary systems around $2 - 3 M_{\odot}$ stars at an epoch similar to the late heavy bombardment. *Hubble Space Telescope* far-ultraviolet spectroscopy strongly suggests ongoing, external metal pollution in two remnant Hyads. For ongoing accretion in both stars, the polluting material has $\log[n(\text{Si})/n(\text{C})] > 0.2$, is more carbon deficient than chondritic meteorites, and is thus rocky. These data are consistent with a picture where rocky planetesimals and small planets have formed in the Hyades around two main-sequence A-type stars, whose white dwarf descendants bear the scars. These detections via metal pollution are shown to be equivalent to infrared excesses of $L_{\text{IR}}/L_{*} \sim 10^{-6}$ in the terrestrial zone of the stars.

Key words: open clusters and associations: individual (Hyades)— stars: abundances— planetary systems— white dwarfs

1 INTRODUCTION

Despite the proliferation of confirmed exoplanets, and continuing successes in novel methods and instruments designed for their detection, planetary systems in star clusters remain elusive. Of the roughly 800 known exoplanets, only *four* are known to orbit stars in clusters. The first two exoplanets identified in clusters were giant planets orbiting giant stars (Sato et al. 2007; Lovis & Mayor 2007); one of those planets (ϵ Tau b) was discovered in the Hyades. This relatively tiny number has only recently doubled with the radial velocity detection of two hot Jupiters around Sun-like stars in Praesepe (Quinn et al. 2012).

This situation is unfortunate because star clusters can, in principle, provide a sound statistical basis for planet population studies. A cluster offers uniform distance, age, and metallicity, and typically has a well-studied mass function and local environment (Cochran et al. 2002). Specifically, clusters allow studies of planet formation as a function of stellar mass, as this is one of the few independent variables, and arguably the most significant. With its super-solar metallicity, the Hyades is an excellent hunting ground for giant planets, but a precision radial velocity survey of nearly 100 solar- and low-mass main-sequence stars resulted

in no detections (Paulson et al. 2004). A similar search of about 90 dwarf, subgiant, and giant stars in M67 also produced no planet candidates (Pasquini et al. 2012). It may be that the lack of planet detections (relative to field stars) is a telltale, and that clusters have an impact on both the planet formation process or their longer-term survival, but a lack of sensitivity due to youthful stellar activity is a distinct possibility for the null results of these radial velocity searches.

Debris disks around cluster stars provides complementary information, indicating the presence of planetesimal populations that are typically Kuiper Belt analogs (Wyatt et al. 2003; Zuckerman 2001; Holland et al. 1998), and sometimes containing the dynamical signatures of planets (Kalas et al. 2005). Several examples of dusty, intermediate- and solar-mass, main-sequence stars have been identified in the Hyades and similarly young open clusters (Urban et al. 2012; Cieza et al. 2008); their (infrared) spectral energy distributions are comparable to those observed toward field stars with circumstellar dust (Su et al. 2006; Bryden et al. 2006), and are thus compatible with outer system, icy planetesimal belts. To date, only the unusually strong and warm infrared excess detected around a solar-mass Pleiad (Rhee et al. 2008) has furnished evidence of debris within the inner planetary system of a cluster star, and supports a picture of a dynamically active, terrestrial planetary system.

* E-mail: jfarihi@ast.cam.ac.uk

† STFC Ernest Rutherford Fellow

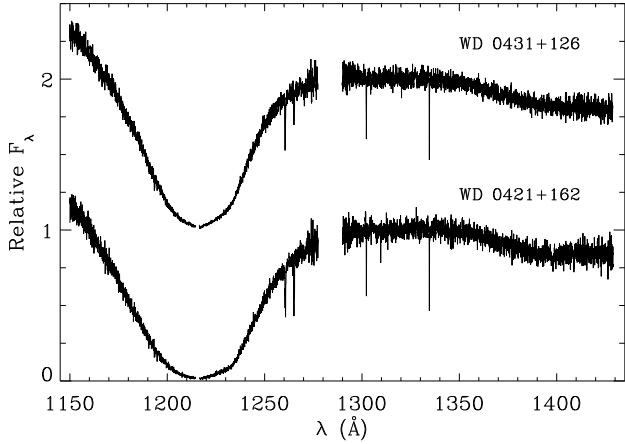


Figure 1. COS spectra of the two white dwarf Hyads. The data have been smoothed by a 5-pixel Gaussian to a resolution near 0.05 \AA (the break in wavelength coverage is due to the gap between detectors). See Figure 2 for feature details and model fits.

This paper reports the detection of silicon-rich material that is consistent with rocky planetary debris around two descendants of intermediate mass (late B- or A-type) stars in the Hyades open cluster. The discovery was made via far-ultraviolet spectroscopy of two white dwarf Hyads: WD 0421+162 (EG 36) and WD 0431+126 (EG 39). The spectra of both stars contain absorption lines of Si II, and upper limits for volatile elements such as carbon, that suggest ongoing accretion from a young but evolved terrestrial planetary system. The observations and data analysis are described in §2, and properties of the planetary debris are discussed in §3, where it is also shown that white dwarf metal pollution is more sensitive than other methods of exo-terrestrial debris detection. Whereas this paper reports the ultraviolet observations of two white dwarf Hyads, Zuckerman et al. (2013, submitted to ApJ) report an optical study of atmospheric metals in Hyades white dwarfs.

2 OBSERVATIONS AND ANALYSIS

2.1 Ultraviolet Spectra

The two Hyads were selected as part of *Hubble Space Telescope* (HST) Cycle 18 Snapshot program 12169 to search for external metal pollution in $17\,000 \text{ K} < T_{\text{eff}} < 25\,000 \text{ K}$ hydrogen-dominated (DA-type) white dwarfs; their cluster membership was incidental. Both stars were observed for 400 s with the Cosmic Origins Spectrograph (COS) using the G130M grating and a central wavelength setting at 1291 \AA , covering $1130 - 1435 \text{ \AA}$. The data were processed and calibrated with CALCOS 2.15.6, and are shown in Figure 1.

The spectra reveal the Stark-broadened Ly α profile intrinsic to DA stars, plus several photospheric lines of Si II. Also visible in each of the spectra are three relatively strong interstellar (resonance) lines, one each of C II, O I, and Si II. In both stars, the latter interstellar line is accompanied by a relatively strong photospheric line, which is significantly red-shifted ($\Delta v \approx 60 \text{ km s}^{-1}$) as to be fully separated from the interstellar component at the instrumental resolution

(Figure 2). Raw signal-to-noise was calculated in the relatively flat region between 1310 and 1330 \AA , yielding 11.4 for 0421+162 and 12.7 for 0431+126.

2.2 Atmospheric Parameters and Metal Abundances

Using available *UBVJ* photometry and the cluster center parallax (Perryman et al. 1998), spectral models were fitted to the measured fluxes and stellar parameters were derived independent of spectroscopy. The effective temperatures and surface gravities calculated in this way are listed in Table 1 and the resulting masses are listed as M_{cl} in Table 2. The most significant source of uncertainty in this method is the parallax, which applies to the cluster core; while the two white dwarfs appear to be well within the central region based on their distance from the core in the plane of the sky, their actual radial offset is relatively uncertain.

The COS spectra were analyzed as detailed in Gänsicke et al. (2012), using the input physics of Koester (2010) but with $\log g$ fixed to the values from the photometry and cluster parallax. Atmospheric parameters determined for both stars from the ultraviolet data are listed in Table 1, where the reported errors are statistical only. Actual errors can be estimated by comparison with previous determinations that use similar or identical models, but are based on optical spectra. There exist several spectroscopic analyses for both 0421+162 and 0431+126, the most recent of which are based on single-order optical spectra (Gianninas et al. 2011), and optical echelle data (Koester et al. 2009); both are listed in Table 1. Overall, there is good agreement between the various methods.

Importantly, it should be emphasized that *the exact choice of T_{eff} and $\log g$ does not significantly alter the derived metal abundances*. The uncertainties give rise to abundance errors smaller than the typical measurement error (0.1 dex), and the metal-to-metal ratios are essentially unaffected (Gänsicke et al. 2012). It is still worthwhile, however, to consider the most accurate white dwarf parameters, as these can be linked to their main-sequence progenitors, and thus provide insight on the rocky planetary systems they construct. The adopted T_{eff} , $\log g$, M_{wd} in Table 2 are the unweighted average of all the independent values listed in Table 1, while M_{sp} is the mass derived from the unweighted average of the two optical spectroscopic datasets. Table 2 also lists main-sequence progenitor masses for the two Hyads, derived using appropriate initial-to-final mass relations (Williams et al. 2009; Kalirai et al. 2008).

The metal absorption features in the COS spectra were analyzed using the T_{eff} and $\log g$ listed at the top of Table 2. Silicon abundance ratios, relative to hydrogen, were calculated for both stars, as well as upper limits for carbon based on several strong lines, including the C II resonance line. From the derived abundances and upper limits, diffusion fluxes were calculated following Gänsicke et al. (2012); these are exactly the accretion rates and limits for each element and are listed in Table 1. This is the correct approach for these warm DA stars, which essentially lack convection zones, and diffusion timescales change as a function of optical depth. In these white dwarfs, the timescale for metals to sink is very short (order of days) and a steady state assump-

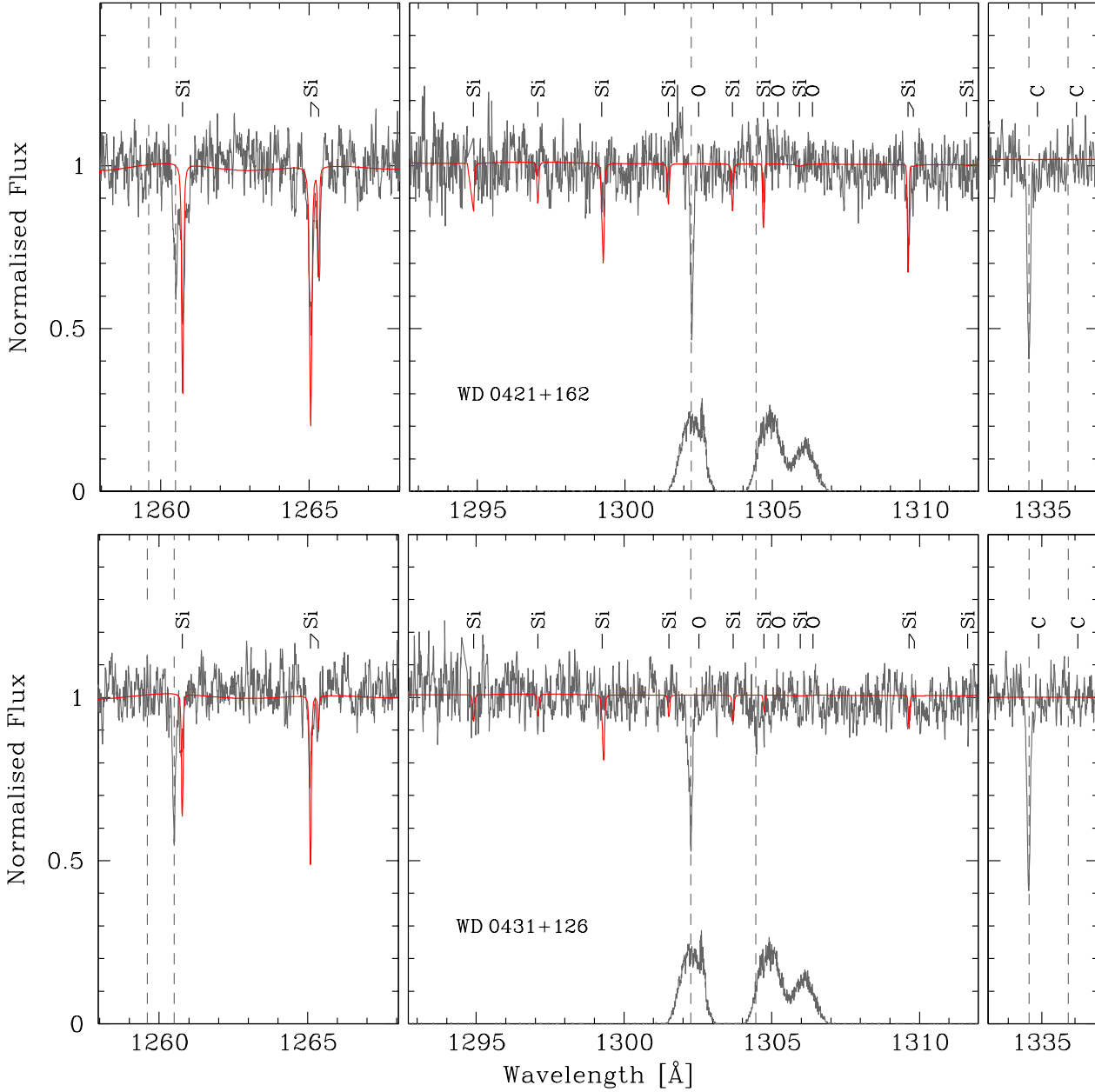


Figure 2. The strongest features detected in the normalized COS spectra (gray) of the two Hyads, together with the best fitting model spectra (red). Photospheric lines of Si II are seen in both stars at vacuum wavelengths 1190.4, 1193.3, 1194.5, 1260.4, 1264.7, 1265.0 Å, while 0421+162 also exhibits 1309.3, 1309.5 Å lines of the same ion. Interstellar resonance lines are present at 1260.4 Å (Si II, but blue-shifted in both stars by 60 km s^{-1} with respect to the corresponding photospheric lines), 1302.2 Å (O I), and 1334.5 Å (C II), and are indicated by dashed lines. Similarly indicated are additional interstellar lines at 1259.5 Å (Si II) and 1335.7 Å (C II) often seen in far-ultraviolet spectra of nearby white dwarfs; their absence here illustrates the low interstellar column density along the line of sight to the cluster. Geocoronal airglow of O I at 1302.2, 1304.9, and 1306.0 Å can contaminate COS spectra to some degree, and typical airglow line profiles are shown in the middle panel scaled to an arbitrary flux.

tion is safe (for a detailed discussion, see Gänsicke et al. 2012).

2.3 Photospheric Velocities and Gravitational Redshifts

Both stars were also observed in the SPY survey (Napiwotzki et al. 2003), on two separate nights each with

UVES, and these spectra were downloaded from the VLT archive and analyzed to search for additional metals lines and to calculate radial velocities. There is no evidence of Ca II K 3933.7 Å or Mg II 4481.2 Å absorption, which are the strongest metal transitions in the optical for white dwarfs in this temperature range. The line velocities of H α and H β (the sum $v_{\text{rad}} + v_{\text{gr}}$) were measured for both stars, in each of their datasets and are listed in Table 2. The measurements

Table 1. Atmospheric Parameters from Photometry and Cluster Parallax, Optical and Ultraviolet Spectroscopy

WD	T_{eff} (K)	$\log g$ (cm s^{-2})	Method
0421+162	18 676(130)	8.05(02)	1
	19 364(40)	8.08(01)	2
	20 010(315)	8.13(05)	3
	18 918(8)	8.05	4
0431+126	21 000(1022)	8.14(06)	1
	20 929(40)	8.09(01)	2
	21 890(346)	8.11(05)	3
	20 992(9)	8.14	4

Method: (1) *UBVJ* photometry combined with cluster parallax; (2) Optical echelle spectroscopy (Koester et al. 2009) with updated models (S2.1); (3) Single-order optical spectroscopy (Gianninas et al. 2011); (4) COS spectroscopy with $\log g$ fixed.

for $\text{H}\beta$ agree within 2% of that found for $\text{H}\alpha$, but the NLTE core of the latter line makes it more reliable and thus only those velocities were used.

Notably, the average, heliocentric-corrected velocities from fits to three Si II lines in the COS spectra of both stars, listed in Table 2, agree remarkably well with the Balmer line velocities, and demonstrate unambiguously that the metal lines are photospheric. The velocities derived from the interstellar C II and Si II lines are consistent with those measured for the local interstellar cloud toward several Hyades stars (Redfield & Linsky 2001).

If both white dwarfs are moving at a radial velocity similar to the cluster center, then their remaining velocity components can be used to establish their masses and radii via gravitational redshifts plus a (theoretical) mass-radius relation (Koester 1987). This is the only available method for deriving single white dwarf masses that does not rely on atmospheric models. The cluster core radial velocity is $+38.6 \text{ km s}^{-1}$, the two stars are 0.9 and 3.4 pc distant from the cluster center in the plane of the sky, and are therefore likely to be within the $r < 10$ pc defined cluster center (Perryman et al. 1998). Gravitational redshifts were derived from the UVES data and white dwarf masses were calculated adopting the cooling models of Holberg & Bergeron (2006) and the mass-radius relations of Panei et al. (2000). Table 2 summarizes the results and yields very similar masses for the two stars, listed as M_{gr} ; these measurements compare favorably to those determined in previous Hyades studies (Claver et al. 2001; Reid 1996; Wegner et al. 1989).

3 RESULTS AND DISCUSSION

3.1 Not Interstellar Matter

Before discussing the implications of detecting photospheric silicon in the COS spectra of these remnant Hyads, it is appropriate to review the arguments against an interstellar origin for these lines. First, while absorption from the local interstellar cloud is detected via the strong 1260.4 Å resonance line, the additional lines at 1264.7 and 1265.0 Å arise from an excited state 0.035 eV above the ground state, which is unpopulated in the interstellar medium, and hence must be

Table 2. Results Summary

WD	0421+162	0431+126
Adopted Parameters:		
T_{eff} (K)	19242(586)	21202(459)
$\log [g \text{ (cm s}^{-2}\text{)}]$	8.09(04)	8.11(03)
Velocities (km s^{-1}):		
$v_{\text{H}\alpha,1}$	74.8(0.6)	73.7(0.6)
$v_{\text{H}\beta,1}$	74.1(1.3)	72.6(1.3)
$v_{\text{H}\alpha,2}$	76.3(0.6)	76.6(0.6)
$v_{\text{H}\beta,2}$	78.1(1.3)	77.2(1.3)
v_{Si}^{\dagger}	77.1	79.0
v_{gr}	37.0(0.6)	36.6(0.6)
Stellar Masses (M_{\odot}):		
M_{cl}	0.65(01)	0.71(04)
M_{sp}	0.69(02)	0.69(02)
M_{gr}	0.70(01)	0.70(01)
M_{wd}	0.67(02)	0.69(02)
M_{ms}	2.5(0.2)	2.7(0.2)
Debris Properties:		
$\log [n(\text{Si})/n(\text{H})]$	-7.5	-8.0
$\log [n(\text{Si})/n(\text{C})]$	> 0.7	> 0.2
$\log [\dot{M}_{\text{Si}} \text{ (g s}^{-1}\text{)}]$	5.3	4.8
$\log [\dot{M}_{\text{Z}} \text{ (g s}^{-1}\text{)}]^{\ddagger}$	6.2	5.6

Note. M_{cl} is the mass derived assuming the cluster parallax, M_{sp} is the mass derived via spectroscopy, M_{gr} is the mass derived by gravitational redshift, M_{wd} is the adopted white dwarf mass, and M_{ms} is the main-sequence progenitor mass. Gravitational redshifts are derived by assuming $v_{\text{rad}} = 38.6 \text{ km s}^{-1}$ (See §2.2 and 2.3 for details).

[†]Errors are a few km s^{-1} .

[‡]Calculated assuming silicon represents 0.16 of the total mass, as in the bulk Earth (§3).

photospheric. Second, if the white dwarfs have accreted interstellar material, one would expect to detect photospheric carbon at Si/C broadly consistent with the solar value. As shown below, the non-detection of carbon implies that infalling debris is at least an order of magnitude higher in Si/C than expected for the interstellar medium. Third, even for the relatively low accretion rate of $\dot{M}_{\text{Si}} = 10^{4.8} \text{ g s}^{-1}$ in 0431+126, the infall of interstellar gas would be dominated by *hydrogen* at $\dot{M}_{\text{H}} \geq 10^{7.8} \text{ g s}^{-1}$. For Eddington type (gravitational) accretion at relative speeds of 40 km s^{-1} this would require $\rho_{\text{H}} \sim 100 \text{ cm}^{-3}$ (Farihi et al. 2010a).

3.2 Can Silicon be Supported by Radiative Levitation?

For DA white dwarfs of $T_{\text{eff}} \approx 20\,000 \text{ K}$, the detection of atmospheric metals has previously been an unambiguous sign of ongoing accretion. Only high levels of metal pollution are detectable with optical spectroscopy of warm DA stars, via calcium or magnesium absorption lines, and the corresponding heavy element masses cannot be radiatively sustained in any atmospheric models (Koester & Wilken 2006). The sensitive ultraviolet data obtained with COS reveal relatively modest levels of atmospheric silicon, an element that could potentially be susceptible to radiative levitation in this range of effective temperatures, unlike calcium and magnesium.

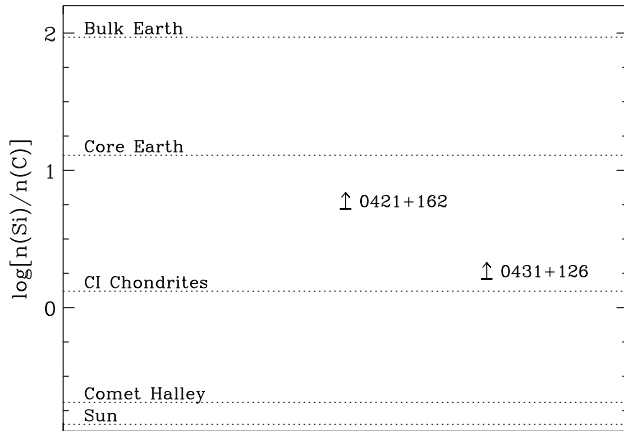


Figure 3. Lower limits to the Si/C abundances in the material polluting the two Hyades white dwarfs, assuming accretion is ongoing. Also shown are the same ratios for the Sun, Halley, chondrites, the core and bulk Earth (Lodders 2003; McDonough 2000; Lodders & Fegley 1998). These lower limits indicate that currently infalling material in both stars must be rocky; the Si/C ratios are more volatile-depleted than those in chondritic meteorites, suggesting formation in the terrestrial zone of their respective planetary systems.

The amount of atmospheric silicon that can be supported by stellar radiation is not known, and previous model comparisons with metals in $T_{\text{eff}} > 25\,000$ K white dwarfs have not yet been quantitatively successful (Chayer et al. 1995b). The only available model at lower temperatures predicts that surface silicon abundances of $[\text{Si}/\text{H}] = -8.0$ are maintained by radiative acceleration at 20 000 K and $\log g = 8.0$ (Chayer & Dupuis 2010); 0421+162 and 0431+126 have $[\text{Si}/\text{H}] = -7.5$ and -8.0 respectively.

However, there are at least three problems with the picture in which silicon is radiatively supported in both of these white dwarfs. First, the *cooler* of the two stars has *more* atmospheric silicon, in contrast to model predictions in which levitation efficiency scales with luminosity. Second, in the full COS Snapshot sample, there are numerous stars in the same temperature range with detected silicon abundances lower than the two Hyads (Gänsicke et al. 2013, in preparation; Koester et al. 2012). Specifically, there are at least 11 stars with measured $[\text{Si}/\text{H}] < -8.0$, and seven of these are predicted to have higher levitation efficiency than both 0421+162 and 0431+126 (Koester et al. 2012). Third, silicon cannot have been supported in the atmosphere of these two white dwarfs for their entire cooling age; near 70 000 K any and all primordial silicon will sink (Chayer et al. 1995a), and thus the silicon must be external. Radiative levitation of silicon is therefore not supported by the data at the observed atmospheric parameters and abundances.

3.3 Super Chondritic Si/C

Figure 3 plots the Si/C number ratio for each of the stars, and compares it to several Solar System benchmarks. The key result is that material being currently accreted must be more carbon-deficient than chondritic meteorites and thus rocky. In contrast, planetary debris that originates in an ex-

trasolar Kuiper Belt analog is expected to have a high fraction of volatiles like carbon, as observed in comets such as Halley (Mumma et al. 1993); during the giant phases of the progenitor star, volatile elements should not be significantly depleted within $r \gtrsim 50$ km planetesimals orbiting beyond 30 AU (Jura & Xu 2010). Thus, planetary material currently being accreted by these two descendants of A-type stars in the Hyades was likely formed in their inner regions, and is thus analogous to asteroidal material, i.e. exo-terrestrial.

The total heavy element accretion rates for the stars, \dot{M}_Z in Table 2, are calculated assuming silicon is 0.16 by mass as in the bulk Earth (McDonough 2000; McDonough & Sun 1995; Allègre et al. 1995), as this has been shown to most closely reflect the total composition where eight or more metals are detected (Zuckerman et al. 2010). These inferred total accretion rates are between 10 and 100 times lower than found for any other DAZ star of similar effective temperature, and this is due to the superior sensitivity of COS ultraviolet data (hence the motivation for the COS Snapshot).

Assuming these stars are accreting calcium and magnesium in bulk Earth proportions relative to silicon, the photospheric abundances would be $[\text{Ca}/\text{H}] = -8.7, -9.3$ and $[\text{Mg}/\text{H}] = -7.3, -7.9$ for 0421+162, 0431+126 respectively. Model spectra calculated with these abundances have Ca II 3934 Å and Mg II 4482 Å line widths around 1 mÅ and would therefore not be detectable with current ground-based facilities. While such detections should be possible with ELTs, the Mg II resonance lines in the near-ultraviolet are predicted to be significantly larger, at 50 – 100 mÅ.

3.4 Rocky Debris Detection: Pollution vs. Infrared Excess

Spitzer studies of metal-enriched white dwarfs have shown that only those circumstellar disks with infall rates above 10^8 gs^{-1} are capable of producing detectable infrared excesses (Farihi et al. 2009; Jura et al. 2007), and the silicon-bearing Hyads keep to this trend. All eight of the classical, single Hyades (super)cluster white dwarfs were observed with cryogenic IRAC – to search for young and still-warm giant planets – but no infrared excesses were detected (Farihi et al. 2008).

For polluted white dwarfs with infrared-detected disks, the thermal F_ν continuum peaks near $5 \mu\text{m}$ from $T \approx 1000$ K dust (Girven et al. 2012; von Hippel et al. 2007), in stark contrast with dusty main-sequence stars such as Vega and β Pic. The white dwarf disks have relatively large fractional infrared luminosities, ranging from 0.001 to 0.03, including at least six stars with $L_{\text{IR}}/L_* > 1\%$ (Farihi et al. 2012, 2010b). The fractional excesses tend towards smaller values with increasing stellar effective temperature (Farihi 2011), possibly due to a smaller available area to un-sublimated dust (Farihi et al. 2012) within the finite Roche limit of the star, where the debris is likely generated by asteroids perturbed onto star-crossing orbits (Veras et al. 2013; Bonsor & Wyatt 2012; Debes et al. 2012; Debes & Sigurdsson 2002), and subsequently tidally disrupted (Jura 2003). These data can be used to estimate L_{IR}/L_* for the two polluted Hyads, by assuming disk mass scales with accretion rate, and extrapolating from infrared detections. Taking $L_{\text{IR}}/L_* \sim 0.001$ for 10^9 gs^{-1} (Farihi

2011) from the known $T_{\text{eff}} \sim 20\,000\text{ K}$ white dwarfs with dust, the corresponding fractional dust luminosities would be $10^{-5.8}$ and $10^{-6.4}$ for 0421+162 and 0431+126 respectively.

Hence, these detections of exo-terrestrial debris via atmospheric metal pollution in white dwarfs are at least as sensitive as equivalent infrared observations of main-sequence stars. For A-type stars, which are the likely progenitors of the two Hyads studied here, $L_{\text{IR}}/L_* \sim 10^{-5} - 10^{-6}$ sensitivities are readily achieved via 24 and $70\ \mu\text{m}$ photometry (Su et al. 2006), but are mainly insensitive to dust within 10 AU (Wyatt 2008). Only a small fraction of main-sequence stars display infrared excesses consistent with warm debris in the terrestrial zones of their host stars (Kennedy & Wyatt 2012; Melis et al. 2010), and by necessity they tend to have spectacular infrared excesses (Rhee et al. 2008; Song et al. 2005). For observations that probe within several AU, such as $12\ \mu\text{m}$ *IRAS* or *WISE* photometry, dust detections typically require $L_{\text{IR}}/L_* \gtrsim 10^{-4}$. As shown above, it is likely that white dwarfs enable detections at least two orders of magnitude smaller than this via pollution, and are thus a highly sensitive probe of terrestrial planetary debris around nearby stars.

4 SUMMARY

Sensitive ultraviolet observations with *Hubble* COS suggest the ongoing accretion of silicate-rich and carbon-poor circumstellar material at two white dwarf descendants of intermediate-mass (A-type) stars in the Hyades open cluster. In each case, currently infalling material is found to be more carbon-deficient than CI chondrites, and consistent with terrestrial-like planetesimals at 625 Myr, which is approximately the timescale of the late heavy bombardment in the Solar System. This evidence supports the idea that these two Hyads had the rocky building blocks necessary for the formation and retention of terrestrial planets.

The study of rocky exoplanetary material via white dwarfs has great potential. It is the only method whereby the bulk composition of entire planetesimals (and possibly large bodies akin to planetary embryos) can be ascertained. Infrared observations can reveal material in the terrestrial zone of nearby stars, but the requirement for large flux excesses – and the dearth of examples despite large searches – implies that white dwarf pollution may already have yielded more detections of material in this region. At least 20% to 30% of cool white dwarfs show evidence for refractory element pollution (Zuckerman et al. 2010, 2003), compared to less than 1% of main-sequence stars with warm debris. In fact, *two of the three nearest white dwarfs are metal-polluted*: vMa 2 and Procyon B (Farihi et al. 2013). The discovery of what are likely rocky planetary systems in the Hyades highlights the power of the archaeological approach to terrestrial exoplanetary science.

ACKNOWLEDGMENTS

The authors thank S. Redfield for useful conversations regarding interstellar matter in the vicinity of the Hyades, and the anonymous referee for comments that improved the

manuscript. Balmer lines in the atmospheric models were calculated with the modified Stark broadening profiles of Tremblay & Bergeron (2009) kindly made available by the authors. This work is based on observations made with the *Hubble Space Telescope* which is operated by the Association of Universities for Research in Astronomy under NASA contract NAS 5-26555. These observations are associated with program 12169. J. Farihi gratefully acknowledges the support of the STFC via an Ernest Rutherford Fellowship, and B. T. Gänsicke was supported by the STFC through a rolling grant at Warwick University.

REFERENCES

- Allègre C. J., Poirier J. P., Humler E., Hofmann A.W. 1995, *Earth Planetary Sci. Letters*, 4, 515
 Bonsor A., Wyatt M. C. 2012, *MNRAS*, 420, 2990
 Bonsor A., Mustill A. J., Wyatt M. 2011, *MNRAS*, 414, 930
 Bryden G., et al. 2006, *ApJ*, 636, 1098
 Cieza L. A., Cochran W. D., Augereau J. C. 2008, *ApJ*, 679, 720
 Cochran W. D., Hatzes A. P., Paulson D. B. 2002, *AJ*, 124, 565
 Chayer P., Fontaine G., Wesemael F. 1995a, *ApJS*, 99, 189
 Chayer P., Vennes, S., Pradhan A. K., Thejll P., Beauchamp A., Fontaine, G., Wesemael F. 1995b, *ApJ*, 454, 429
 Chayer P., Dupuis J. 2010, in K. Werner, T. Rauch eds., *American Institute of Physics Conference Series*, 1273, 394
 Claver C. F., Liebert J., Bergeron P., Koester D. 2001, *ApJ*, 563, 987
 Debes J. H., Sigurdsson S. 2002, *ApJ*, 572, 556
 Debes J., Walsh K., Stark C. 2012, *ApJ*, 747, 148
 Farihi J. 2011, in Hoard D. W. ed., *White Dwarf Atmospheres and Circumstellar Environments*. Wiley-VCH, Berlin (ISBN 978-3-527-41031-6), 117
 Farihi J., Barstow M. A., Redfield S., Dufour P., Hambly N. C. 2010a, *MNRAS*, 404, 2123
 Farihi J., Becklin E. E., Zuckerman B. 2005, *ApJS*, 161, 394
 Farihi J., Bond H. E., Dufour P., Haghighipour N., Schaefer G., Holberg J., Barstow M. A., Burleigh M. R. 2013, *MNRAS*, in press
 Farihi J., Gänsicke B. T., Steele P. R., Girven J., Burleigh M. R., Breedt E., Koester D. 2012, *MNRAS*, 421, 1635
 Farihi J., Jura M., Lee J. E., Zuckerman B. 2010b, *ApJ*, 714, 1386
 Farihi J., Jura M., Zuckerman B. 2009, *ApJ*, 694, 805
 Farihi J., Zuckerman B., Becklin E. E. 2008, *ApJ*, 674, 431
 Gänsicke B. T., Koester D., Farihi J., Girven J., Parsons S. G., Breedt E. 2012, *MNRAS*, 424, 333
 Gianninas A., Bergeron P., Ruiz M. T. 2011, *ApJ*, 743, 2011
 Girven J., Brinkworth C. S., Farihi J., Gänsicke B. T., Hoard D. W., Marsh T. R., Koester D. 2012, *ApJ*, 749, 154
 Holberg J. B., Bergeron P. 2006, *AJ*, 132, 1221
 Holland W. S., et al. 1998, *Nature*, 392, 788
 Jura M. 2003, *ApJ*, 584, L91

- Jura M., Farihi J., Zuckerman B. 2007, *ApJ*, 663, 1285
- Jura M., Xu S. 2010, *AJ*, 140, 1129
- Kalas P., Graham J. R., Clampin M. 2005, *Nature*, 435, 1067
- Kalirai J. S., Hansen B. M. S., Kelson D. D., Reitzel D. B., Rich R. M., Richer H. B. 2008, *ApJ*, 676, 594
- Kennedy G. M., Wyatt M. C. 2012, *MNRAS*, 426, 91
- Koester D. 1987, *ApJ*, 322, 852
- Koester D. 2010, In *Memorie della Societa Astronomica Italiana*, 81, 921
- Koester D., Voss B., Napiwotzki R., Christlieb N., Homeier D., Lisker T., Reimers D., Heber U. 2009, *A&A*, 505, 441.
- Koester D., Wilken D. 2006, *A&A*, 453, 1051
- Koester D., Gänsicke B. T., Girven J., Farihi J. 2012, in *Proceedings of the 18th White Dwarf Workshop* (arXiv:1209.6036)
- Lodders K. 2003, *ApJ*, 591, 1220
- Lodders K., Fegley B. 1998, *The Planetary Scientist's Companion* (New York: Oxford University Press)
- Lovis C., Mayor M. 2007, *A&A*, 472, 657
- McDonough W. F. 2000, in Teisseyre R., Majewski E., eds, *Earthquake Thermodynamics and Phase Transformation in the Earths Interior*. Academic Press, San Diego, p.5
- McDonough W. F., Sun S. S. 1995, *Chemical Geology*, 120, 223
- Melis C., Zuckerman B., Rhee, J. H., Song, I. 2010, *ApJ*, 717, L57
- Mumma M J., Weissman P. R., Stern S. A. 1993, in Reipurth V. B., Jewitt D., Keil K., eds., *Protostars and Planets III*. University of Arizona Press, Tucson, p. 1177
- Napiwotzki R., et al. 2003, *Msngr*, 112, 25
- Panei J. A., Althaus L. G., Benvenuto O. G. 2000, *A&A*, 353, 970
- Paulson D. B., Cochran W. D., Hatzes A. P. 2004, *AJ*, 127, 3579
- Pasquini L., et al. 2012, *A&A*, 545, A139
- Perryman M. A. C., et al. 1998, *A&A*, 331, 81
- Quinn S. N., et al. 2012, *ApJ*, 756, L33
- Redfield S., Linsky J. 2001, *ApJ*, 551, 413
- Reid I. N. 1996, *AJ*, 111, 2000
- Rhee J. H., Song I., Zuckerman B. 2008, *ApJ*, 675, 777
- Sato B., et al. 2007, *ApJ*, 661, 527
- Song I., Zuckerman B., Weinberger A. J., Becklin E. E. 2005, *Nature*, 436, 363
- Su K. Y. L., et al. 2006, *ApJ*, 653, 675
- Tremblay P. E., Bergeron P. *ApJ*, 696, 1755
- Urban L. E., Rieke G., Su K., Trilling D. E. 2012, *ApJ*, 750, 98
- Veras D., Mustill A. J., Bonsor A., Wyatt M. C. 2013, *MNRAS*, in press (arXiv:1302.3615)
- von Hippel T., Kuchner M. J., Kilic M., Mullally F., Reach W. T. 2007, *ApJ*, 662, 544
- Wegner G., Reid I. N., McMahan R. K. 1989, in G. Wegner, ed., *White Dwarfs*. Springer, New York, p. 378
- Williams K. A., Bolte M., Koester D. 2009, *ApJ*, 693, 355
- Wyatt M. C. 2008, *ARA&A*, 46, 339
- Wyatt M. C., Holland W. S., Greaves J. S., Dent, W. R. F. 2003, *Earth, Moon, and Planets*, 92, 423
- Zuckerman B. 2001, *ARA&A*, 39, 549
- Zuckerman B., Koester D., Reid I. N., Hüensch M. 2003, *ApJ*, 596, 477